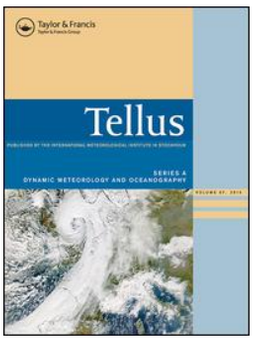

Tellus A: Dynamic Meteorology and Oceanography

ISSN: (Print) 1600-0870 (Online) Journal homepage: https://www.tandfonline.com/loi/zela20

Investigation of processes governing the large-scale variability of the atmosphere using low-order barotropic spectral models as a statistical tool

Harald A. Kruse & K Hasselmann

To cite this article: Harald A. Kruse & K Hasselmann (1986) Investigation of processes governing the large-scale variability of the atmosphere using low-order barotropic spectral models as a statistical tool, Tellus A: Dynamic Meteorology and Oceanography, 38:1, 12-24, DOI: 10.3402/tellusa.v38i1.11694

To link to this article: https://doi.org/10.3402/tellusa.v38i1.11694

Tellus (1986), *38A*, 12–24

Investigation of processes governing the large-scale variability of the atmosphere using low-order barotropic spectral models as a statistical tool

By HARALD A. KRUSE and K. HASSELMANN, *Max-Planck-Institut für Meteorologie, Bundestrasse 55, 2000-Hamburg 13, F.R. Germany*

(Manuscript received January 10; in final form May 13, 1985)

ABSTRACT

Idealized low-order spectral models based on quasi-geostrophy have been proposed by Charney, Egger, and others for a qualitative explanation of quasi-stationary flow patterns in the troposphere, such as blocking highs. To test these concepts, we consider spectral, quasi-geostrophic, barotropic models of a slightly higher, but still relatively low resolution (28 and 68 degrees of freedom). The models are treated as regression models, the predictors being the individual components of the prognostic vorticity equation, namely the beta, advection, orography, friction and forcing terms. A 10-year record of observed north-hemispheric geopotential data is used as data basis for the statistical regression analysis. The regression model may be interpreted as a truncated model in which the individual terms have been modified by (a) projecting the truncation and other systematic model errors onto the terms retained in the simplified system, and (b) keeping in the retained terms only the contributions which are correlated with the observed change in the atmospheric state. The model is applied in the inverse mode as a diagnostic tool to determine which processes are most important for the evolution of the system, and how much of the observed large-scale variance of the atmosphere can be explained by such a low-order system. Despite the strong spectral truncation, the model is found to explain a reasonable percentage of the observed variance (of the order of 30%, or 0.55 correlation, for 68 components). However, it was not possible to explain a significant fraction of the variance by still more strongly truncated models of the idealized form proposed by Charney and Egger. Our analysis indicates that all degrees of freedom of the truncated system (28 or 68) contribute significantly to the dynamics of the large-scale components. The most important processes are the wave/mean-flow interaction and the beta effect, followed by the nonlinear interactions among waves and the annually varying thermal forcing. Interactions with orography and frictional effects are generally negligible. The residual variance not represented by the model cannot be parameterized in a simple manner in terms of the components of the truncated model itself and must be treated as external stochastic forcing. Thus for a realistic description of large-scale atmospheric variability, low-order spectral models must be augmented by a significant stochastic forcing component in addition to the internal interactions.

1. Introduction

A basic question in understanding the low frequency atmospheric variability on time scales of several days to a few months is the rôle played by the internal interactions between large-scale atmospheric components, as compared with the external forcing exerted by other slowly varying components of the climate system, such as the ocean. In the present paper, we try to gain some insight into the nature of internal large-scale atmospheric interactions.

For the study of the dynamics of the atmosphere, complex general circulation models (GCMs) of the type applied in operational weather forecasting are generally used. These models include realistic representations of as many physical processes as possible, are therefore expensive, and

permit only a limited number of experiments. The restrictions in the statistical data base of these experiments often make it difficult to determine whether all processes represented in the models are significantly correlated with the behaviour of the real atmosphere.

On the other hand, many qualitative features of low-frequency global atmospheric variability appear already in the solutions of strongly simplified versions of the general hydro-thermodynamic equations. Thus the frequency-wavenumber variance spectra of observed atmospheric anomalies agree fairly well with the dispersion relations of free waves computed for a system linearized about a realistic mean flow (Ahlquist, 1982; Kasahara, 1980; Machenhauer, 1977). Simplified models for the linear and nonlinear response to orographic and thermal forcing proposed by Egger (1978), Charney and DeVore (1979), Charney and Strauss (1980), Charney et al. (1981) and others, or models of low-order nonlinear vacillations by Lorenz (1960), Platzman (1962), and Baer (1970) also appear to qualitatively reproduce the principal features of observed low-frequency vacillations.

The purpose of this paper is to determine through a quantitative statistical comparison with observations the degree to which the low-frequency variability of the atmosphere can indeed be explained in terms of such relative elementary models. As model we shall use the equivalent-barotropic vorticity equation with orographic interactions and Newtonian forcing. It was a beta-plane version of this model, with very low spectral truncation, which was proposed by Egger to explain the development of blocking highs, and by Charney and collaborators to describe the alternating blocked and zonal flow states of the index cycle. We shall use models of slightly higher resolution containing 4 meridional wavenumbers and a (rhomboidal) truncation at zonal wavenumber $m = 3$ or 8 (corresponding to 28 and 68 degrees of freedom, respectively).

The overall skill of the models is established in the usual manner by correlating the time series of the observed and predicted atmospheric states, or changes of atmospheric state, for different forecast times. To determine the relative contribution of different processes to the skill, the observed atmospheric change is also correlated with the individual model terms. The basic data set consists of the 10-year twice-daily gridded data of analysed hemispheric 500 hPa geopotential height observations (Section 2), which were kindly provided by the Deutscher Wetterdienst (German Weather Service) and transformed to a spherical surface harmonics (SSH) representation by the Institute of Meteorology at the University of Köln (Speth and Kirk, 1981). From this, we derived the "observed" stream function data by means of the quasi-geostrophic balance equation on the sphere.

The truncated model (Section 3) is not used directly, but is regarded as a generalized statistical regression model in which the individual dynamical terms are treated as predictors and the (integrated) model tendency as the predictand. Thus the coefficients of the individual terms are adjusted to achieve an optimal prediction. In this manner, the truncation and other errors of the model are projected onto the terms retained in the truncated system, and the components of the nonresolved residual processes which are correlated with the resolved processes are included implicitly in the model (Section 4). It should be pointed out that the method emphasizes the ability of the model to predict changes of the atmospheric state, and is therefore not appropriate for a discussion of the force balances characterizing very low frequency or stationary atmospheric waves.

A similar but simplified statistical analysis, using a linear rather than a full nonlinear model, has recently been carried out by Roads and Barnett (1984) for the same data set. The present approach has been extended by Bruns (1985) to a baroclinic model. Bruns uses a slightly different dynamical description in terms of the atmospheric anomaly fields rather than the complete atmospheric state. He also applies an alternative statistical analysis method in the frequency rather than the time domain, which permits a discussion of the zero-frequency stationary wave components.

In Section 5, we compare the overall skill of our model with the two extreme cases of a simple persistence model and a high resolution GCM. The contributions of the individual processes, and the effects of truncation, are discussed in Section 6. The results are summarized in Section 7.

2. Data base

Our basic data consists of northern hemispheric analyses of the geopotential height ϕ provided by

the German Weather Service (Deutscher Wetterdienst), Offenbach. The field ϕ is given on a rectangular grid (381 × 381 km² at 60°N) on a stereographic plane at 60° N (with the centre of projection at the South Pole), covering the area north of about 10 ... 12.5°N. The data are recorded for 6 pressure levels 850, 700, 500, 300, 200, 100 hPa, but for our purposes we have used only the 500 hPa data. The analyses are provided twice daily at 00.00 and 12.00 GMT, and cover the 10-year period 1967–1976, corresponding to a time series of length $2 \times 365 \times 10 = 7{,}300$ for each grid point.

For estimates of statistical significance, we assume that the number of independent samples is approximately 600. This is based on a conservative estimate of 6 days for the autocorrelation time of the spherical harmonic expansion coefficients (for most components, the autocorrelation time scale is considerably smaller). All statistical significance evaluations given in the following refer to 95 % confidence levels.

The grid point data were converted to (complex) spectral coefficients ϕ_n^m by least square fitting the spherical surface harmonic (SSH) expansion

$$\phi(\lambda, \theta, p, t) = \sum_{\substack{m=0 \\ (n-m=\text{even})}}^{15} \sum_{n=m}^{15} \mathrm{Re}[\phi_n^m(p, t) \cdot e^{im\lambda}] \cdot p_n^m(\theta) \tag{2.1}$$

to the finite set of grid points. The series was limited to meridionally symmetric modes ($n - m$ = even) and truncated triangularly at the total wavenumber $n = 15$, yielding a set of $(n + 1) \cdot (n + 2)/2 = 136$ real coefficients (Speth and Kirk, 1981).

The geopotential data were slightly modified in order to satisfy the boundary condition $\partial\phi/\partial x = 0$ at the equator. The longitude dependence in the tropical regions was also smoothed by requiring

$$\phi(\lambda, \varphi = 0°) = \frac{1}{2\pi} \int_0^{2\pi} \times \phi(\lambda, \varphi = 12.5°\mathrm{N}) \cdot \mathrm{d}\lambda = \text{const.} \tag{2.2}$$

This was found to be necessary in order to reduce the noise in the lowest order stream function (rigid body rotation) component ψ_1^0 derived from the geopotential height data. (The association of the noise in ψ_1^0 with the extrapolation to the equator was pointed out by W. Metz and D. Schilling, personal communication.) The time series of the geopotential SSH coefficients and the recombined height field charts in the data covered region were not visibly influenced by this smoothing procedure.

The geopotential height was converted to the "observed" stream function ψ by the linear balance equation for the sphere,

$$\mathrm{div}\,(f \cdot \mathrm{grad}\,\psi) = \nabla^2 \phi, \tag{2.3}$$

which relates the non-divergent geostrophic wind to the geopotential field ϕ. The solution for ψ, which is antisymmetric with respect to the equator, was obtained by expanding eq. (2.3) in spherical surface harmonics (cf. Eliasen and Machenhauer, 1969).

The orographic data required for the model were based on a set of global terrain height (and sea depth) on a 1° × 1° grid provided by the Geophysical Fluid Dynamics Laboratory, NOAA (Smith et al., 1965). After averaging over 5° longitude × 2.5° latitude areas and setting sea depths equal to zero, the expansion in SSHs was performed with the same truncation as for the ϕ and ψ data.

3. The dynamical model

The dynamical model is based on the familiar quasi-geostrophic vorticity equation for the stream function ψ, formulated in pressure and spherical coordinates,

$$\frac{\partial}{\partial t} \nabla^2 \psi = J(\psi, \nabla^2 \psi + f) + f_0 \frac{\partial \omega}{\partial p} \tag{3.1}$$

together with the heat balance equation, which relates the pressure velocity ω to the stream function ψ,

$$\omega = -\frac{f_0}{\sigma} \cdot \left[J\left(\psi, \frac{\partial}{\partial p} \psi\right) + \frac{\partial}{\partial t} \frac{\partial}{\partial p} \psi - Q \right]. \tag{3.2}$$

Here Q is a heating function and σ represents the static stability. The Coriolis parameter f is regarded as variable in the vorticity advection term in eq. (3.1), but is kept fixed at a constant mid-latitude value f_0 in the remaining terms of the equations.

From a scale analysis viewpoint, the model (3.1), (3.2) is strictly consistent only in the β-plane, for flow scales small compared with planetary dimensions (cf. Pedlosky, 1979, and Kruse, 1983). We nevertheless follow the standard practice of applying the model also to planetary scales, since it

represents the simplest energetically consistent model and a fully scale-consistent nonlinear model would require a considerably more cumbersome analysis, for example in terms of Hough functions (cf. Kasahara, 1976). The model has been widely used as the basis for formulating simple hypotheses of the type we wish to test.

For the upper boundary, we assume a freely moving, impermeable pressure surface p_2,

$$\omega(p_2) = 0. \tag{3.3}$$

At the lower boundary, taken at a constant pressure surface p_1, the pressure velocity is determined by the time derivative of the surface pressure, Ekman pumping, thermal forcing and orographic interactions. In the linear approximation, the boundary condition takes the form

$$\omega(p_1) = \left[\rho f_0 \frac{\partial}{\partial t} \psi - \mu_E f_0 \nabla^2 \psi + \mu_E \mu_\varphi \nabla^2 \varphi - J(\psi, h) \right]_{\text{at } p = p_1} \tag{3.4}$$

The thermal forcing function φ represents the total heat released into the atmosphere below the lower model boundary $p = p_1$ and consists of a superposition of the sensible heat flux from the earth and sea surface to the boundary layer and the diabatic heating within the boundary layer. The horizontal inhomogeneity of the density distribution within the boundary layer induced by thermal expansion modifies the divergence of the Ekman transport and thus the Ekman suction term (cf. Egger, 1978; Charney and De Vore, 1979). For our purposes, it is sufficient to note that thermal heating represents an external forcing function, independent of ψ.

To derive the barotropic, spectral form of the model, the vertical and horizontal structure of the stream function ψ is expanded in a set of orthonormal modes,

$$\psi(\lambda, \theta, p, t) = \sum_\alpha \sum_i \psi^i_\alpha(t) \cdot F^i(p) \cdot Y_\alpha(\lambda, \theta) \tag{3.5}$$

Here the functions Y_α denote the antisymmetric spherical surface harmonics (SSH) and the functions F^i an orthonormal set of vertical structure functions, which we need not specify further. We assume here only that the first "barotropic" mode ($i = 1$) is approximately constant with height.

Substitution of the expansion (3.5) into (3.1)–(3.4) and projection onto the first vertical mode $\psi^1_\nu \equiv \psi_\nu$ and the truncated set of wavenumbers $\gamma = (m_\nu, n_\nu)$ then yields the truncated spectral model

$$\dot{\psi}_\nu = B_\nu + A^0_\nu + A^w_\nu + O_\nu + E_\nu + F^0_\nu + F^a_\nu + N_\nu \tag{3.6}$$

with source terms as follows:

B_ν = linear β-term = $L_\nu \psi_\nu$, where

$$L_\nu = \frac{i2\Omega m_\nu}{\nu_\nu},$$

$$\nu_\nu = n_\nu(n_\nu + 1),$$

$$\Omega = 2\pi/(1 \text{ day}).$$

(Inclusion of the divergence terms in the barotropic mode yields a modified operator $L'_\gamma = L_\gamma \cdot \nu_\gamma/(\nu_\gamma + \Lambda^2)$, where Λ^2 is the Lamb parameter. However, we shall retain first the simpler expression L_γ and consider the Lamb parameter corrections later in the context of the regression analysis.)

A^0_ν = nonlinear wave/mean-flow interaction term = $\sum_{\alpha,\beta} J_{\alpha\beta\gamma} \psi_\alpha \cdot \psi_\beta$, with m_α and/or $m_\beta = 0$.

A^w_ν = nonlinear wave-wave interaction term = $\sum_{\alpha,\beta} J_{\alpha\beta\gamma} \psi_\alpha \psi_\beta$ with m_α and $m_\beta \neq 0$.

The interaction coefficients occurring in A^0_γ and A^w_γ are given by

$$J_{\alpha\beta\gamma} = \frac{-\nu_\beta}{\nu_\gamma} \cdot a^{-2} I_{\alpha\beta\gamma},$$

with $I_{\alpha\beta\gamma} = \int\int_{\text{sphere}} J(Y_\alpha, Y_\beta) Y_\gamma \mathrm{d}(\cos\theta)\mathrm{d}\lambda$, where a is the radius of the earth, J denotes the Jacobian and Y_α a (normalized) SSH function.

O_γ = orography interaction term = $\sum_\alpha H_{\alpha\gamma} \psi_\alpha$, where

$$H_{\alpha\gamma} = \frac{-2\Omega}{\nu_\gamma} \sum_\beta h_\beta I_{\alpha\beta\gamma},$$

and h_β denotes the SSH expansion coeffiecient of $h/RT \cdot g^{-1}$ = orography/scale height.

E_ν = Ekman friction term = $K_\nu \psi_\nu$ (K_ν real, constant).

F^0_γ = mean heat flux term = $(f_0/p_1)\mu_E \mu_\varphi \varphi_\gamma$ = const.

F^a_ν = seasonal modulation of heat flux term = $F^c_\gamma \cos \omega_0 t + F^s_\gamma \sin \omega_0 t$, F^c_γ = const, F^s_γ = const, $\omega_0 = 2\pi/1$ year.

The symbols L, J, H, K denote constants involving the Rossby speed, nonlinear interaction coefficients, orography, and the friction coefficient, respectively. They depend on the wavenumbers α,

β, γ and are theoretically prescribed. The residual term N_ν denotes the nonlinear truncation error and consists of quadratic products involving terms with vertical wavenumbers greater than unity or horizontal wavenumbers beyond the truncation limits. Truncation errors arise also in the boundary conditions, horizontally through the orography term, and vertically by neglecting the baroclinic modes in the forcing terms of the lower boundary condition.

We choose a rhomboidal truncation, appropriate for our emphasis on mid-latitudes, $n_\nu - m_\nu \leqslant K$, $m_\nu \leqslant M$, with $K = 7$ (corresponding to four odd modes $n - m = 1, 3, 5$ and 7) and $M = 3$ or 8, resulting in a total of $\frac{1}{2}(K + 1)(2M + 1) = 28$ or 68 degrees of freedom, respectively.

For the following, we write eq. (3.6) in the abbreviated form

$$\dot{\psi}(t) = \sum_q X^q[\psi(t)] + N, \tag{3.7}$$

where the SSH wavenumber index γ has been dropped throughout, ψ is understood as the vector of all SSH components of the barotropic mode, and the sum over q represents the sum over the 8 terms of eqn (3.6).

Since we shall be interested in the change of states over a time period of $\tau = 1 \ldots 10$ days, we shall consider also the integrated form of (3.7), which we write formally as

$$y(t) \equiv \psi(t + \tau) - \psi(t) = \sum_q \int_t^{t+\tau} \{X^q[\psi(t')] + N\}\, dt' \equiv \sum_q x^q(t, \tau) + n. \tag{3.8}$$

4. Statistical-dynamical model

The objective of our analysis is to test how well a model of the type (3.8) is able to describe the observed behaviour of plantetary-scale flow fields, and to determine the relative contributions of the different processes to the evolution of the real atmosphere.

For this purpose, we extend our model equations (3.8) to the more general linear form

$$y(t) \equiv \psi(t + \tau) - \psi(t) = \sum_q c^q \cdot x^q + n(t). \tag{4.1}$$

The constant coefficients c^q are regarded here as free regression coefficients which we determine from the data by minimizing the residual noise n. For a perfect model, all regression coefficients c^q would be unity, the total correlation of the set of predictors x^q with the predictand $y(t)$ would also be unity, and the residual noise n would vanish. In practice, we will find $c^q \neq 1$ (generally < 1) and the total correlation is less than unity, because the model contains various sources of errors resulting in a finite noise n. The principal errors arise from the truncation, the quasi-geostrophic approximation, the approximations at the upper and lower boundaries and the parameterizations of the effects of friction and heating.

To the extent that they are correlated with the source terms x^q of the truncated system, the errors can be automatically compensated for by adjusting the regression coefficients c^q to minimize n. For this reason, the regression coefficients may in principal become greater than unity. However, in most cases the coefficients are found to be smaller than the theoretical value of unity. This could be due to the fact that the errors are negatively correlated with the source terms, but is more probably due to unavoidable errors in computing the source terms x^q from the data.

For the regression analysis, the predictors $x^q(t, \tau)$ are determined by integrating the empirical source functions X^q as computed from the observed data over the interval τ in accordance with eq. (3.8). The model is used in this mode purely as a dynamical diagnostic tool, not for prediction. The skill achieved by the model in the diagnostic mode will generally be considered larger than the skill of the same model used in the forecast mode, where the source functions are evaluated from the predicted atmospheric state computed by the model from the given initial state. Most of the results discussed in the following apply to diagnostic mode integrations.

With the exception of the thermal forcing term, the model is regarded as time independent (i.e. constant regression coefficients) and the data as statistically stationary. In view of the expected strong seasonality of the thermal forcing, however, this term is represented in terms of three regression coefficients as the sum $F_\gamma = F_\gamma^0 + F_\gamma^a$ of a constant term F and an annual modulation F_γ^a represented by its two lowest harmonic components (cf. eq. (3.6)).

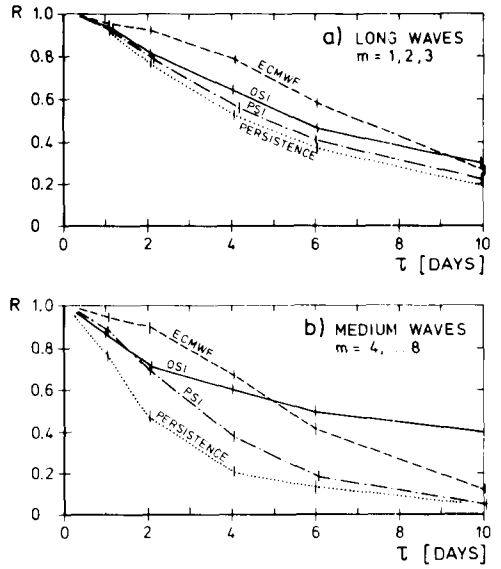

Fig. 1. Pattern correlation R for 500 hPa geopotential anomaly as function of forecast interval τ for long waves $m = 1, 2, 3$ (panel a) and medium waves $m = 4 \ldots 8$ (panel b). The curves OSI and PSI refer to integrations of the moderately truncated model (4 meridional components, 9 zonal components, including $m = 0$) with the observed and predicted source functions, respectively. The prediction run was carried out with the regression model determined from an OSI run with $\tau = 1$ day. The ECMWF curves refer to forecasts with the operational T63 model.

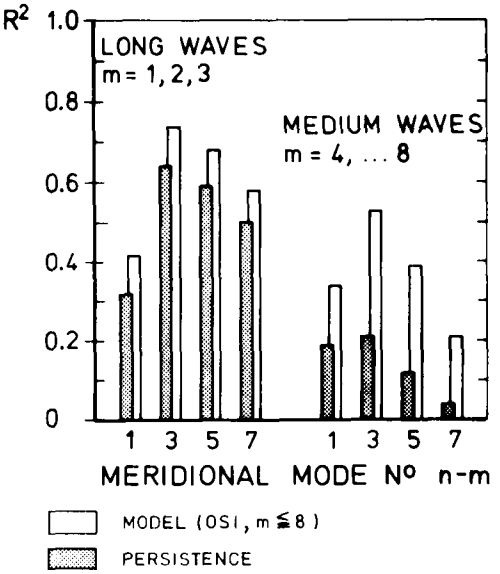

Fig. 2. Squared correlation of observed and predicted state for $\tau = 2$ days for long and medium zonal waves, decomposed with respect to the four meridional components $n - m = 1, 3, 5$ and 7. Model results refer to diagnostic runs with the moderately truncated model ($m \leqslant 8$).

5. Model skill

An indication of the skill attainable with a low-order spectral barotropic model is given by Fig. 1, which shows the pattern correlation of the observed and model 500 hPa fields as a function of forecast time τ for the long wave ($m = 1, 2, 3$) and medium wave ($m = 4, \ldots 8$) components of the field. The results refer to the 68-component model and both filtered fields contain all four meridional wavenumber components. Model integrations were made both in the diagnostic mode (OSI = observed source function integrals) and forecast mode (PSI = predicted source function integrals). In the diagnostic mode, the regression coefficients were determined anew for each integration interval τ. For the forecast integration, the regression coefficients were determined from an OSI run with $\tau = 1$ day. As expected, the correlation is higher for the diagnostic mode than the forecast mode, particularly for large τ.

Also shown for comparison are the correlations achieved with a simple persistence model, in which the initial state is assumed to remain unchanged, and with the operational high resolution global GCM of the European Centre for Medium Range Weather Forecasts, in the forecast mode (ECMWF Forecast Reports, 1980).

The model skill (fraction of variance computed by the model) is given by the correlation squared. Fig. 2 shows the corresponding variance for the low-order dynamic model and persistence model, decomposed into the 4 meridional wavenumbers, at $\tau = 2$ days. Of interest is the increase in variance explained by the model beyond the persistence level. (It can be inferred from Fig. 1 and is shown explicitly in Fig. 3 below that this is approximately independent of τ for the diagnostic mode.)

For the long waves, most of the forecast skill of the low-order model derives simply from persistence. The additional variance attributable to the low order spectral dynamics is of the order of only 10% for the diagnostic mode. The high resolution

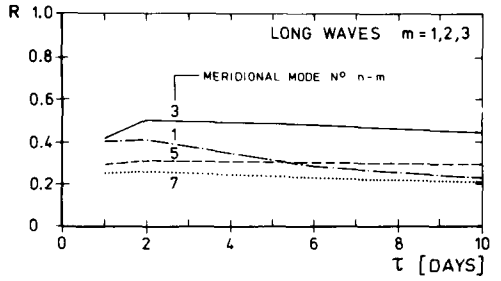

Fig. 3. Change-of-state correlation R for the long zonal wave components ($m = 1, 2, 3$), separated into the four meridional modes $n - m = 1, 3, 5, 7$, for the moderately truncated model ($m \leqslant 8$).

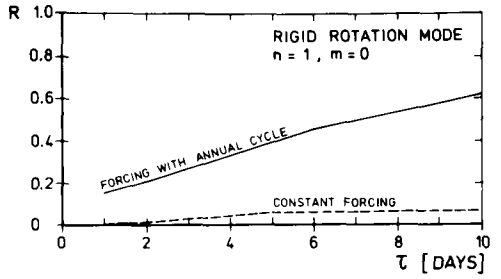

Fig. 4. Change-of-state correlation R for the rigid rotation mode ($m = 0$, $n = 1$) for the moderately truncated model ($m \leqslant 8$) with and without annual cycle in external forcing term.

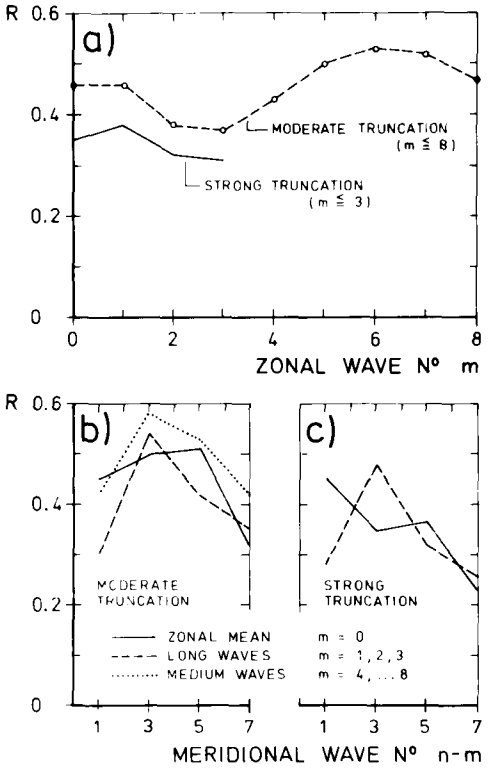

Fig. 5. Change-of-state correlation for $\tau = 6$ days as a function of zonal and meridional wavenumbers. Panel (a) refers to the superposition of all 4 meridional wavenumbers, panels (b) and (c) to the separate superposition patterns for medium-, long-wave and zonal mean components. Both moderately and strongly truncated models are shown.

ECMWF forecast model yields significantly higher values, for example, 23% predicted dynamical variance above the 13% persistence contribution for $\tau = 6$ days. The large contribution from persistence reflects simply the strength of the large scale quasi-stationary wave patterns. For the still more slowly varying zonal flow components ($m = 0$, not shown), the persistence contribution is still larger.

For the medium waves, the additional variance computed from the low order dynamics is significantly larger, typically of order 20–30%, and exceeds the persistence contribution for τ greater than 2 days. At $\tau = 5$ days, for example, the diagnostic model and the ECMWF forecast model both yield approximately 30% explained variance (0.55 correlation), of which only 2% is attributable to persistence.

Since the models were tuned with respect to the predicted change of state of the atmosphere, rather than the state of the atmosphere itself, it is useful to express the overall model skill also in terms of the computed change. In this case, of course, the persistence model yields zero skill.

Fig. 3 shows the change-of-state pattern correlations as a function of τ for the superposition of the three longest zonal waves ($m = 1, 2, 3$), separated into the four meridional constituents ($n - m = 1, 3, 5, 7$). The model was integrated in the diagnostic mode (as in all cases discussed in the following) and was truncated at $m = 8$. The weak τ dependence evident in Fig. 3 is found also for the medium zonal components ($m = 4 - 8$) and the zonal flow components $m = 0$. An exception is the lowest, rigid body rotation mode $m = 0$, $n = 1$ which shows a marked increase of R with τ arising from the annual cycle forcing term, cf. eq. (3.6), (Fig. 4).

Fig. 5 shows an alternative representation of the correlation between the computed and observed

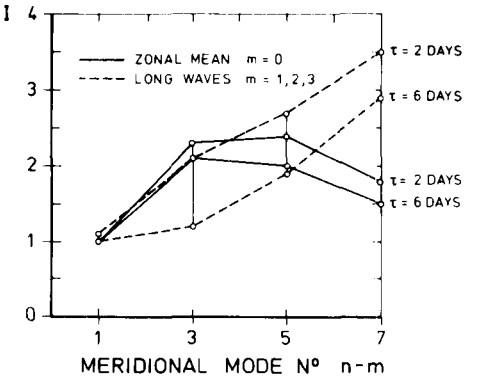

Fig. 6. Ratio $I = R^2$ (moderate truncation)/R^2 (strong truncation) of change-of-state variance predicted by moderately and strongly truncated models for long zonal waves and zonal mean flow, decomposed into meridional modes.

change of state as a function of zonal and meridional wavenumber for $\tau = 6$ days. The medium waves are again seen to have the highest correlation. The correlation levels of order 0.5 for the moderate truncation model ($m \leqslant 8$) imply computed dynamic variance contributions of the order of 25 %, which are consistent with the results shown in Figs. 1 and 2. Also shown are the correlation values achieved with the more strongly truncated model ($m \leqslant 3$). The ratios $I = R^2(m \leqslant 8)/R^2(m \leqslant 3)$ of the explained variance achieved with the moderately and strongly truncated spectral model are shown in Fig. 6 for the long waves and zonal mean flow (medium waves are not resolved in the strongly truncated model). The increase in I is due primarily to the improved representation of the non-linear wave-wave interaction term and increases, as to be expected, with the meridional mode number. The truncation effect is surprisingly small for the first meridional mode.

6. Contributions of individual processes

We now consider the relative contributions of the different processes of eq. (3.6) to the change-of-state correlation R, or skill R^2. The skill is preferable to the correlation in the present context, since we may consider then the additive contributions to the variance from different processes. However, since the processes are not statistically independent, we must distinguish between the variance contributed by a single process without inclusion of other processes (individual correlation), and the incremental variance contributed through the introduction of a process after the remaining processes have already been represented in the model (partial correlation). The discussion in the following is based on a hierarchy of models in which the processes are introduced sequentially, and we consider then the (partial) variance contribution of each additional process in the hierarchy. We choose the sequence corresponding to the ordering of terms given in eq. (3.6), anticipating that this will correspond also to the relative importance of the processes. However, it must be kept in mind that the successive variance contributions of the individual processes will generally be smaller than the individual variance contributions because of the correlation of the newly added processes with processes already introduced previously. This applies particularly to the quasi-linear term A_0 describing the interaction with the zonal mean flow, which is generally strongly correlated with the β-term B (cf. also Bruns, 1985).

The variance contributions of the different processes for the moderate truncation model $m \leqslant 8$ are summarized in Fig. 7 for different meridional and zonal wavenumbers for an integration time $\tau = 6$ days. Approximately the same variance contributions are found for all τ in the range $\tau = 2 - 10$ days, in accordance with the weak τ-dependence of the total variance shown in Fig. 3.

For the medium waves (zonal wavenumbers $m = 4 - 8$) the full model explains about 30 % of the variance for the 2nd and 3rd meridional mode, and about 15 % for the 1st and 4th modes. The explained variance is fairly evenly partitioned among the β-effect, the interaction with the zonal mean flow, and the wave-wave interaction term. The thermal and orographic forcing and the linear feedback (Eckman friction) are relatively insignificant.

For the long waves ($m = 1 - 3$) more than 60 % of the explained variance can again be attributed to the β-effect, the mean flow advection and wave-wave interactions. The rest is due mainly to the thermal forcing, while the orographic and frictional term are again very small.

The zonal mean flow ($m = 0$) shows characteristics similar to the long waves, except that the

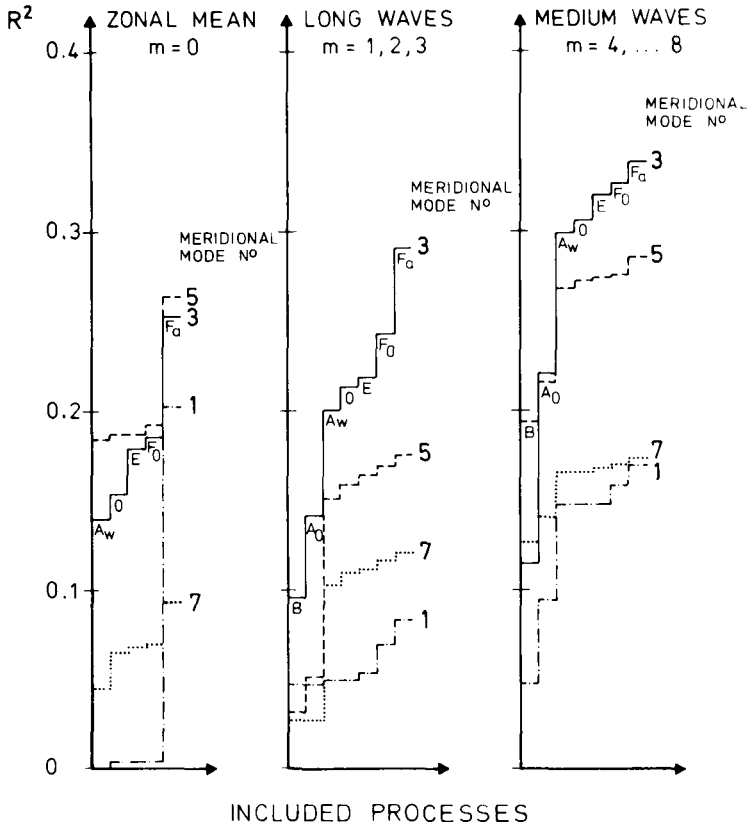

Fig. 7. Fraction of explained variance for a hierarchy of models constructed by sequentially introducing the seven source terms listed in eq. (3.6). The results refer to the moderately truncated model ($m \leqslant 8$) for an integration time $\tau = 6$ days.

β-term and the wave-mean flow interactions are missing in this case.

The regression coefficients generally fall off with increasing τ. Fig. 8 shows as example the decrease of the β-term coefficient c^B for different meridional wavenumbers for the case of the strongly truncated model ($m \leqslant 3$). The decrease in the coefficients essentially balances the increase in the ratio of the variance of the integrated source function to the variance of the change of state. For large τ, the integrated source function variance grows linearly in τ, in accordance with a random walk process, while the change of state variance becomes constant. The resultant explained variance remains at approximately the same level (Fig. 3).

We note that c^B does not begin with the theoretical value of unity near $\tau \to 0$. Since the linear β-term contains no truncation error or parameterization approximation, we attribute this

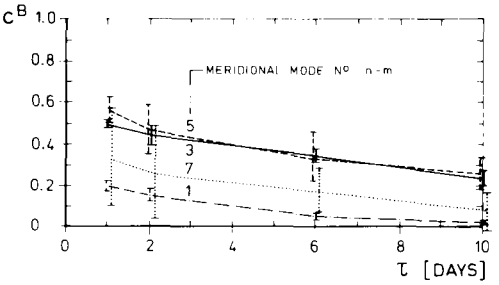

Fig. 8. Dependence of the regression coefficient c^B for the β-term on integration time τ for the strongly truncated model ($m \leqslant 3$). Vertical bars indicate variations between different zonal wavenumbers for a given meridional wavenumber.

to the errors caused by the quasi-geostrophic approximation for large scale planetary flows, which slow down the effective phase velocities of

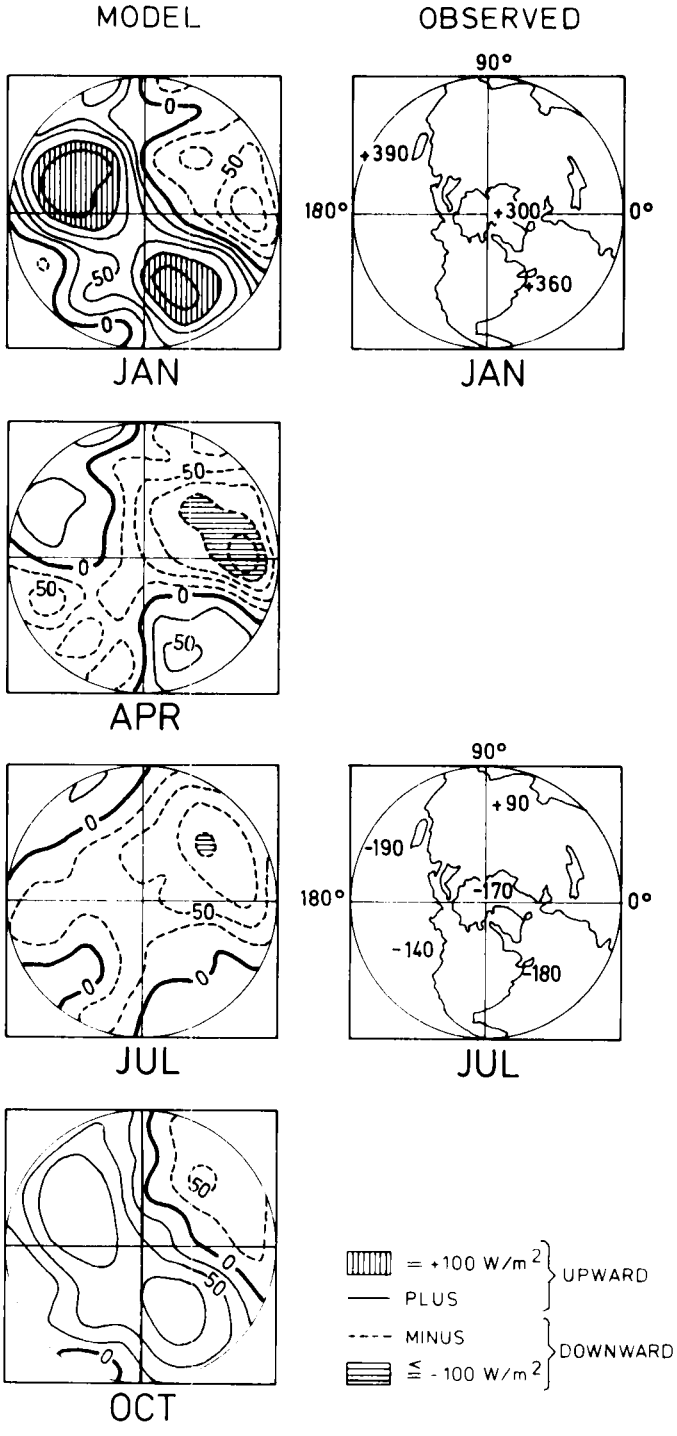

Fig. 9. Net heat flux north of 12.5°N. Left-hand side: inferred from model regression analysis; right-hand side: observations, from Schutz and Gates (1971, 1972).

the planetary scale components (cf. Machenhauer, 1977; Ahlquist, 1982). The values of c^B shown in Fig. 8 are consistent with the orders of magnitude of the Lamb parameter Λ^2 normally introduced to describe this effect. (To relate c^B to the Lamb parameter we note that c^B represents the ratio of the Rossby speed with and without the Lamb parameter correction, respectively, cf. Section 3.)

If the remaining regression coefficients are normalized by c^B to remove this common correction factor, the coefficients for the wave-mean flow and wave-wave interaction are found to be close to unity, as expected, and show no significant dependence on τ. However, the normalized orographic forcing coefficients c^0/c^B are typically only of order 0.1, suggesting that the theoretical barotropic orographic forcing is largely masked, possibly by baroclinic components. The regression coefficients for the weak linear (Ekman or other) forcing terms are also found to be strongly scattered, often changing sign, and are not statistically significant for most modes. The lack of significant linear forcing is consistent with the finding of Egger and Schilling (1983) that the synoptic scale interactions, which appear as external forcing terms in low order spectral models, are not linearly correlated with the larger scale components and can be regarded as statistically independent stochastic (red noise) forcing terms.

These qualitative features are largely insentitive to the truncation of the model, which affects only the magnitude of the total explained variance (cf. Fig. 6) rather than the relative importance of the different processes.

The only significant boundary forcing found was the term $F_\nu(t) = (f_0/p_1)\,\mu_E\,\mu_\varphi\,\varphi_\nu$. It is of some interest to test whether the inferred heat input φ is consistent with standard concepts on the distribution of atmospheric heating. Fig. 9 shows the distribution $\varphi(\lambda, \theta)$ computed from the model for the four seasons, with a suitably chosen factor $\mu_E\,\mu_\varphi$ (a simple boundary layer calculation indicates that the factor is consistent with usual estimates of the Ekman friction and thermal diffusion coefficients in the boundary layer, cf. Kruse, 1983). Also shown are some computations of the total heat flux for January and July from observations by Schutz and Gates (1971, 1972). The inferred heating distribution is not inconsistent with observations, the model reproducing in particular the pronounced warming over the oceans during the winter season.

7. Conclusions

From our diagnostic analysis of the processes governing the dynamics of barotropic large scale planetary flow, we conclude that:

(1) Hypotheses suggesting that barotropic planetary scale motions can be treated qualitatively as a separate dynamical system, whose vacillations can be largely explained by the interactions within the system itself, are not borne out by the observations. The percentage variance of the change of state of the planetary scale motions which can be explained by the interactions within the system itself is relatively low for the lowest order model and increases continuously as the truncation limit is increased. The variance explained by the model is typically of the order of 15% for the most strongly truncated 28 component model (4 meridional, 4 zonal wavenumbers, including $m = 0$) and 30% for the 68 component model (4 meridional, 9 zonal wavenumbers), while the corresponding value for the high resolution ECMWF model (T63, 4096 components) is estimated to lie in the range 70–90% (exact numbers are not available for the application of the ECMWF operational model in the diagnostic rather than the predictive mode). The explained variance remains relatively constant in the forecast range $\tau = 2 - 10$ days. This is a characteristic of diagnostic as opposed to predictive models. The analysis of Bruns (1985) indicates that essentially the same conclusions hold for an extended low-order model including baroclinic modes.

(2) A better simulation of the change of state is generally achieved with low-order spectral models for the medium scale components (meridional wavenumbers 3, 5, zonal wavenumbers 4–8) than for the longest waves.

(3) Thermal forcing was found to be the only significant (deterministic) forcing. The seasonal and geographical distributions inferred for this term are reasonably consistent with the standard picture of atmospheric heating. Interactions with orography and frictional damping were found to be negligible.

(4) The fact that no statistically significant linear feedback terms were found implies in particular that the truncated nonlinear interactions cannot be parameterized in terms of a

(diagonal) linear operator, for example in the form of an effective viscosity or diffusion process. This supports similar findings by Egger and Schilling (1983).

(5) The three processes representing the internal dynamics which were resolved explicitly in the low-order vorticity balance—the β-term, advection by the zonally average flow and wave-wave interactions—were generally of comparable order.

(6) The relative significance of the different terms of the model discussed in (3), (4) and (5) refers to the contributions of the terms to the change of state of the atmosphere, not to the rôle of the terms in the balance of forces characterizing the stationary wave components. (Interactions with orography, for example, are known to be important for the stationary components, although they were found to be negligible in our analysis.) The study of very low frequency variability requires a somewhat different approach in which the emphasis is placed on the force balance rather than the imbalance considered here (cf. Bruns, 1985) and the rôle of slowly varying boundary conditions (SST, snow and ice cover) is explicitly taken into account.

(7) The projection of truncation and other model errors onto the terms included explicitly in the model through the generalized regression analysis did not significantly alter the model coefficients. This suggests that the terms not resolved explicitly in the model should be represented as statistically independent stochastic forcing terms, as also proposed by Egger and Schilling (1983).

In summary, the most appropriate low-order dynamical description of the barotropic planetary scale motions is that of an internally coupled system driven by a superposition of a seasonally dependent external heating and stochastic forcing. For the moderately truncated model ($m \leqslant 8$) and integration times τ in the range 2–10 days, the stochastic forcing contributes about twice as much to the variance of the change of state of the atmosphere as the deterministic internal and external forcing. This ratio increases to 5 : 1 for the strongly truncated model ($m \leqslant 3$). We conclude that although low-order spectral models of the atmosphere are clearly useful tools for studying basic interaction processes, they can provide realistic descriptions of true atmospheric variability only if augmented by significant external stochastic forcing terms.

REFERENCES

Ahlquist, J. E. 1982. Normal-mode global Rossby waves: theory and observations. *J. Atmos. Sci. 39*, 193–202.

Baer, F. 1970. Analytic solutions to low-order spectral systems. *Arch. Meteorol., Geophys., Bioklimatol. A 19*, 255–282.

Bruns, T. 1985. On the contribution of linear and nonlinear processes to the long term variability of large scale atmospheric flows. *J. Atmos. Sci.* (in press).

Charney, J. G. and De Vore, J. G. 1979. Multiple flow equilibria in the atmosphere and blocking. *J. Atmos. Sci. 36*, 1205–1216.

Charney, J. G. and Strauss, D. M. 1980. Form-drag instability, multiple equilibria, and propagating planetary waves in baroclinic, orographically forced, planetary wave systems. *J. Atmos. Sci. 37*, 1157–1176.

Charney, J. G., Shukla, J. and Mo, K. C. 1981. Comparison of a barotropic blocking theory with observation. *J. Atmos. Sci. 38*, 762–779.

ECMWF Forecast Reports Nos. 1 through 12, 1980. European Centre for Medium Range Weather Forecasts, Reading, UK.

Egger, J. 1978. Dynamics of blocking highs. *J. Atmos. Sci. 35*, 1788–1801.

Egger, J. and Schilling, H.-D. 1983. On the theory of the long-term variability of the atmosphere. *J. Atmos. Sci. 40*, 1073–1085.

Eliasen, E. and Machenhauer, B. 1969. On the observed large-scale wave motions. *Tellus 21*, 149–166.

Kasahara, A. 1976. Normal modes of ultra-long waves in the atmosphere. *Mon. Wea. Rev. 104*, 669–690.

Kasahara, A. 1980. Effect of zonal flows on the free oscillations of a barotropic atmosphere. *J. Atmos. Sci. 37*, 917–929.

Kruse, H. 1983. A statistical-dynamical low-order spectral model for tropospheric flows. Hamburg: Hamburger Geophysikalische Einzelschriften, *A59*. (Available from the author.)

Lorenz, E. N. 1960. Maximum simplification of the dynamical equations. *Tellus 12*, 243–254.

Machenhauer, B. 1977. On the dynamics of gravity oscillations in a shallow water model, with applications to normal mode initialization. *Beitr. Phys. Atmos. 50*, 253–271.

Pedlosky, J. 1979. *Geophysical fluid dynamics*, Springer, 624 pp.

Platzman, G. W. 1962. The analytical dynamics of the spectral vorticity equation. *J. Atmos. Sci. 19*, 313–328.

Roads, J. O. and Barnett, T. P. 1984. Forecasts of the 500 mb height using a dynamically oriented statistical model. *Mon. Wea. Rev. 112*, 1354–1369.

Schutz, C. and Gates, W. L. 1971. Global climatic data for surface, 800 mb, 400 mb: January. R-915-ARPA. Santa Monica, California: The Rand Corporation.

Schutz, C. and Gates, W. L. 1972. Global climatic data for surface, 800 mb, 400 mb: July. R-029-ARPA. Santa Monica, California: The Rand Corporation.

Smith, S. M., Menert, H. W. & Sharman, G. 1965. Worldwide ocean depth and continental elevations averaged for areas approximating 1° squares of latitude and longitude. Scripps Institution of Oceanography, Ref. Rep. 65–8, La Jolla, California.

Speth, P. and Kirk, E. 1981. Representation of meteorological fields by spherical harmonics. *Meteorol. Rundsch. 34*, 5–10.